

17 flow, ϕ - azimuthal angle of particle and Ψ_n is the azimuthal angle of the n^{th} -order event
 18 plane [2, 3]. Anisotropic flow coefficient v_n can be used to quantitatively describe the
 19 azimuthal anisotropy. The n^{th} -order flow coefficients can be calculated as $v_n = \langle \cos[n(\phi -$
 20 $\Psi_n)] \rangle / \text{Res}\{\Psi_n\}$, where averaging is performed over all particles and events and $\text{Res}\{\Psi_n\}$ is
 21 resolution of the n^{th} -order event plane. Elliptic (v_2) and triangular (v_3) flow coefficients are
 22 the dominant signals and have been studied at top RHIC and LHC energies [4, 5].

23 In these proceedings, we present measurements of triangular flow of identified particles
 24 (π^\pm , K^\pm , p , \bar{p}) in 0%-60% central Au+Au collisions at $\sqrt{s_{NN}} = 11.5, 14.5, 19.6, 27, 39,$ and
 25 62.4 GeV from the STAR experiment at RHIC.

26 II. DATA ANALYSIS

27 In this work, the data of Au+Au collisions collected from the beam energy scan (BES)
 28 program at RHIC were used. Data set with collision energy of 27 GeV was taken from the
 29 BES-II program (2018) and other energies ($\sqrt{s_{NN}} = 11.5, 14.5, 19.6, 39, 62.4$ GeV) from
 30 BES-I program. Events with minimum bias trigger were selected. Vertex position from the
 31 center of Time Projection Chamber (TPC) along the beam direction (V_Z) was required to
 32 be within ± 40 cm for $\sqrt{s_{NN}} = 39, 62.4$ GeV, ± 50 cm for $\sqrt{s_{NN}} = 11.5$ GeV and ± 70 cm for
 33 other energies. Primary vertex radial position in the transverse direction ($V_r = \sqrt{X^2 + Y^2}$)
 34 was required to be within 2 cm (1 cm for 14.5 GeV). In addition due to shift of the beam
 35 along Y direction in 2014 for 14.5 GeV the V_r cut was applied relative to the beam center
 36 (0.0 cm, -0.89 cm).

37 Only primary tracks were used for event plane reconstruction and collective flow calcu-
 38 lation. It was required that all tracks have number of fit points in TPC larger than 14, and
 39 ratio number of hit points to maximum possible number of hits ($N_{\text{hits}}/N_{\text{poss}}$) is larger than
 40 0.5. The distance of closest approach (DCA) of track to the event vertex was required to be
 41 less than 1 cm for identified particles. All tracks are required to be within a pseudorapidity
 42 range $|\eta| < 1$. Particle identification was carried out using the information about ionization
 43 energy losses (dE/dx) in TPC and m^2 from time-of-flight system (TOF).

44 For measurements of collective flow, the event plane method was used [3]. Tracks from
 45 TPC were divided in two pseudorapidity intervals: east and west (east $-1 < \eta < -0.05$
 46 and west $0.05 < \eta < 1$). Event planes were estimated in each sub-events for each collision

47 centrality. To reduce the impact of nonflow effect (decay of resonances, HBT correlation,
 48 and jets), η -gap ($\Delta\eta$) of 0.1 was required between sub-events. Recentering and shifting
 49 corrections were applied for each event planes due to limited acceptance of the TPC [6].
 50 Resolution of event plane was calculated using two sub-events method [7]. Event plane
 51 resolution for the second and third harmonics are shown on Figs. 1 and 2 as a function of
 52 collision centrality.

53 III. RESULTS

54 Results of elliptic and triangular flow for 0%-60% central Au+Au collisions as a function of
 55 p_T are presented in Figs. 3 and 4 for positively and negatively charged particles, respectively.
 56 Values of v_3 were multiplied by 2.5 for better visualisation. The mass ordering is observed
 57 at low p_T range smaller than 1.5 GeV/ c and the meson-baryon splitting is seen for p_T larger
 58 than 2 GeV/ c . It is seen that triangular flow shows similar features to that of elliptic flow
 59 [8–11].

60 Figures 5 and 6 show v_2 and v_3 scaled with the number-of-constituent quarks (NCQ).
 61 This results are presented as a function of $(m_T - m_0)/n_q$ where m_T is transverse mass, m_0
 62 is particle mass and n_q is the number of constituent quarks. Values of v_3 were multiplied by
 63 2.5. Triangular flow values seem to follow the NCQ scaling. It is seen that (anti)protons,
 64 pions, and kaons follow the same curve for each energy.

65 The $\sqrt{s_{NN}}$ -dependence of difference of triangular flow between positively and negatively
 66 charged particles is presented in Fig. 7 for 0%-60% centrality. The difference increases
 67 with decreasing collision energy. Absolute value of $v_3(X) - v_3(\bar{X})$ is larger for protons and
 68 antiprotons than for pions and kaons. The similar trends were observed for elliptic flow in
 69 Refs. [12, 13] for 0%-80% and 10%-40% central Au+Au collisions.

70 IV. SUMMARY

71 We have presented measurements of triangular flow of identified particles (π^\pm , K^\pm , p, \bar{p})
 72 in 0%-60% central Au+Au collisions at $\sqrt{s_{NN}} = 11.5, 14.5, 19.6, 27, 39, \text{ and } 62.4$ GeV from
 73 the STAR experiment at RHIC. Triangular flow as a function of transverse momentum shows
 74 similar features to that of v_2 , namely the mass ordering and the meson-baryon splitting. The

75 number-of-constituent quark (NCQ) scaling was studied. The NCQ scaling holds better for
76 higher energies. The v_3 difference of particles and antiparticles was presented as a function
77 of $\sqrt{s_{NN}}$. The difference increases with decreasing collision energy.

78

ACKNOWLEDGMENTS

79 The reported study was funded by the Ministry of Science and Higher Education of
80 the Russian Federation, Project “Fundamental properties of elementary particles and cos-
81 mology” No. 0723-2020-0041., and by the MEPhI Program Priority 2030. The work was
82 partially performed using resources of the heterogeneous computing platform HybriLIT of
83 JINR (LIT) (<http://hlit.jinr.ru>) and NRNU MEPhI high-performance computing center.

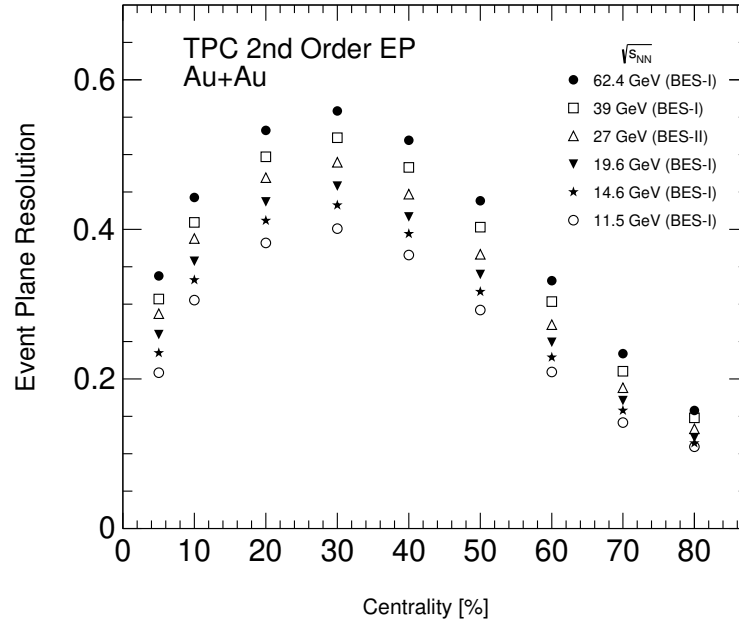


FIG. 1. Event plane resolution of the second harmonic as a function of collision centrality for different energies.

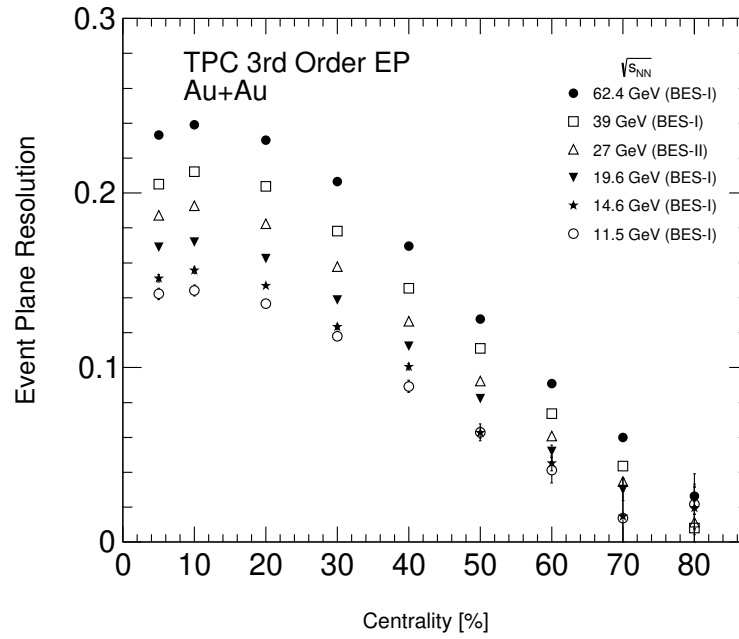


FIG. 2. Event plane resolution of the third harmonic as a function of collision centrality for different energies.

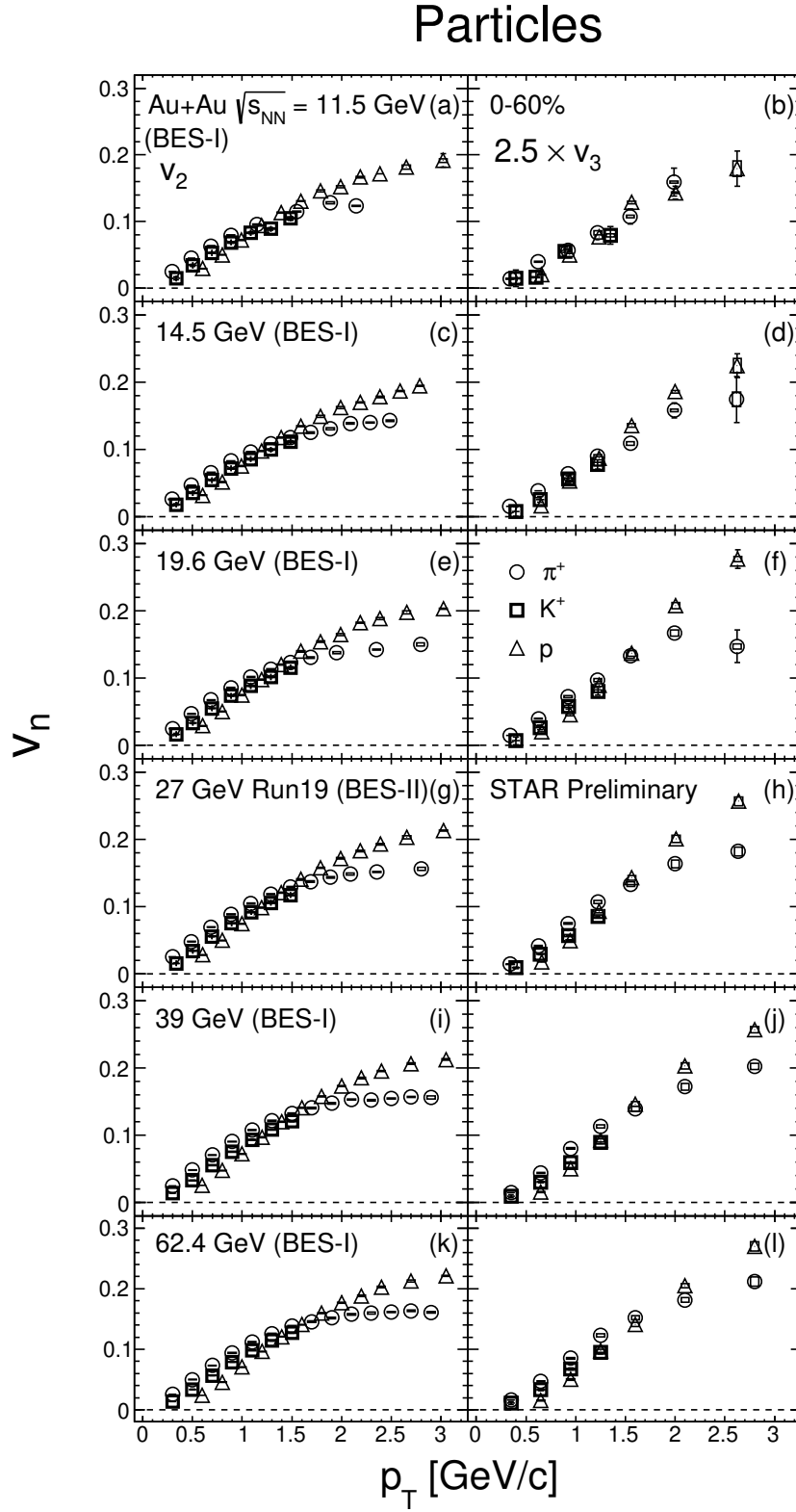


FIG. 3. p_T dependence of elliptic (left) and triangular (right) flow of positively charged particles for 0%-60% central Au+Au collisions for different energies.

Antiparticles

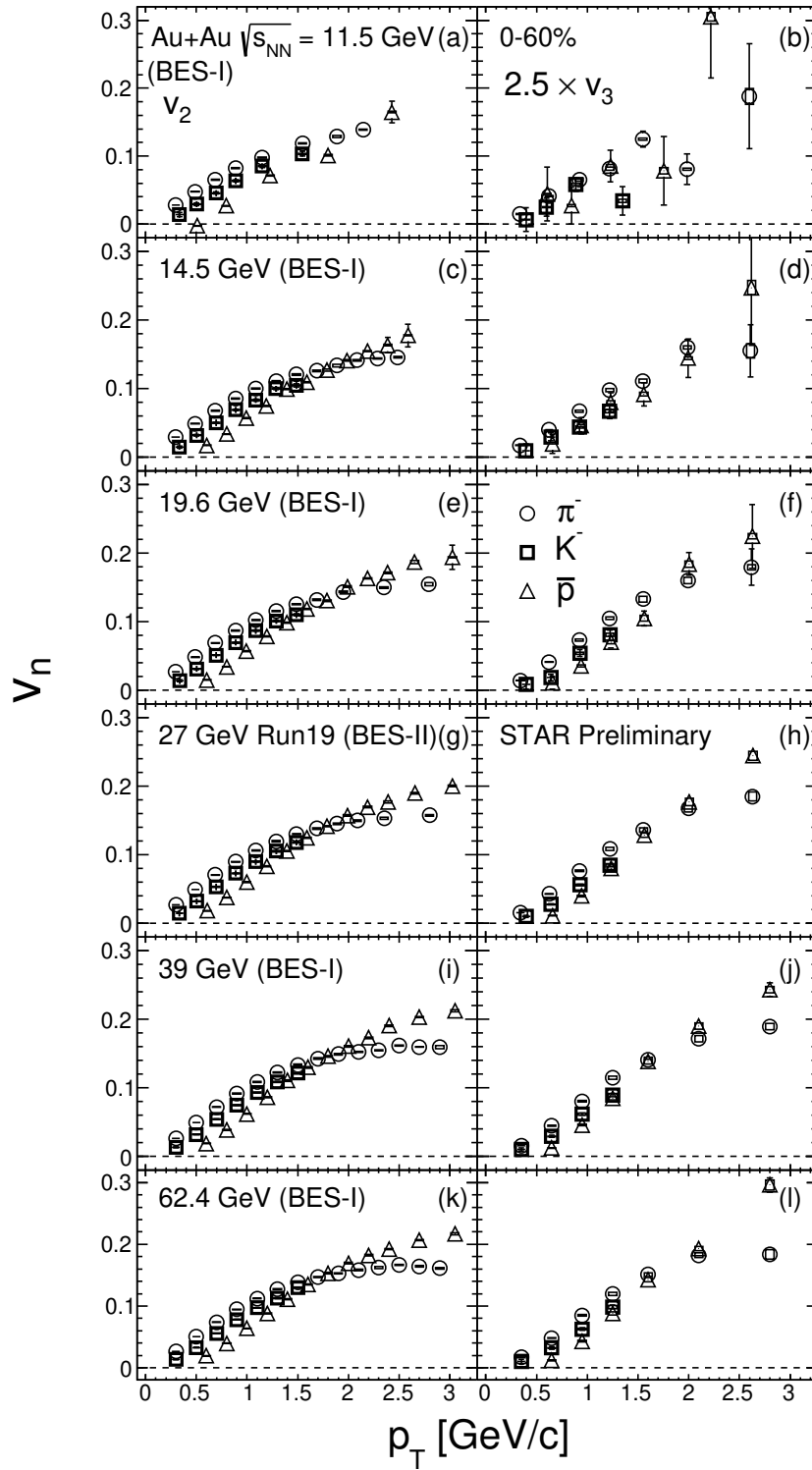


FIG. 4. p_T dependence of elliptic (left) and triangular (right) flow of negatively charged particles for 0%-60% central Au+Au collisions for different energies.

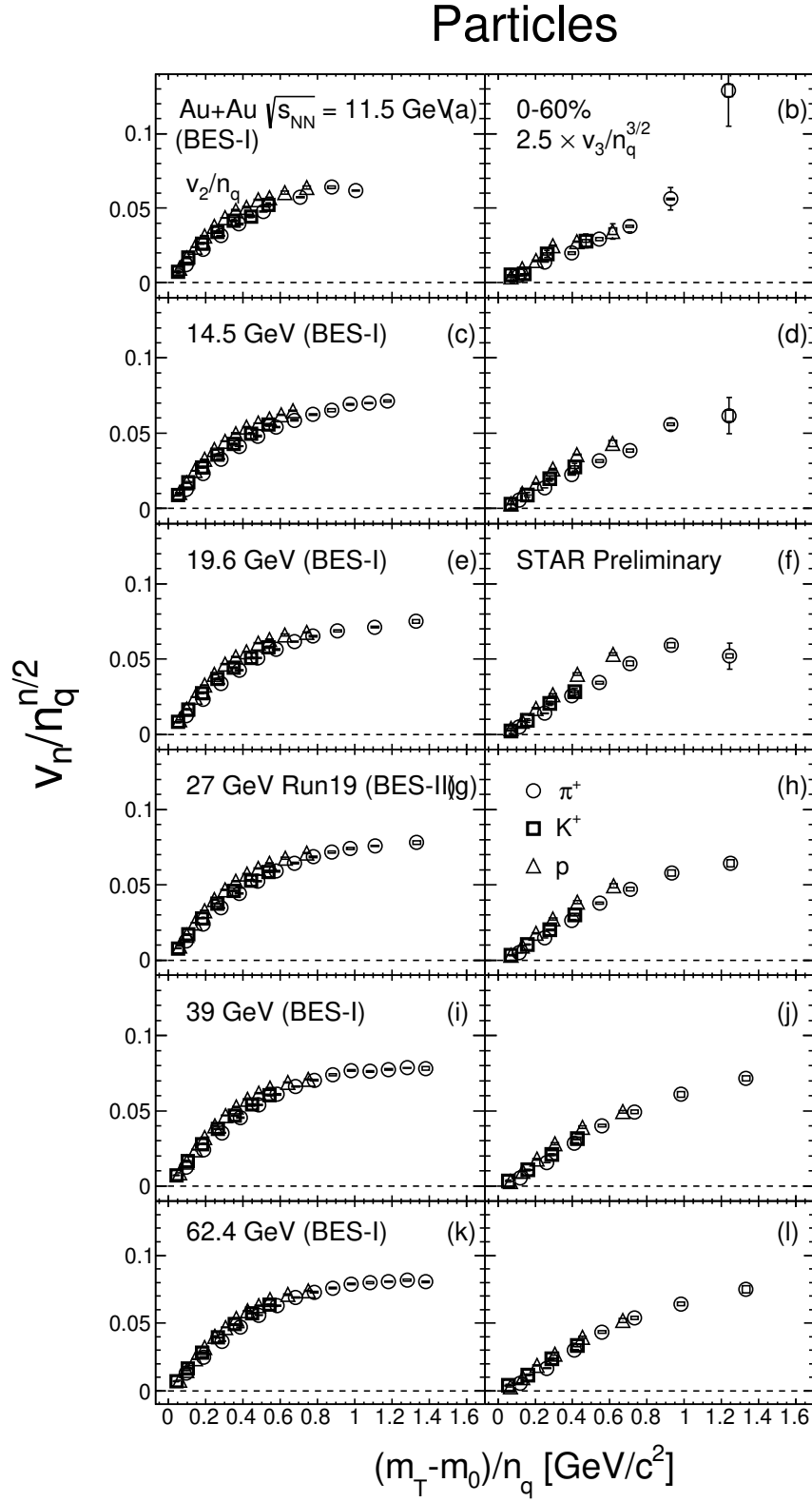


FIG. 5. The number-of-constituent quark (NCQ) scaled v_2 and v_3 of positively charged particles for 0%-60% central Au+Au collisions and six energies.

Antiparticles

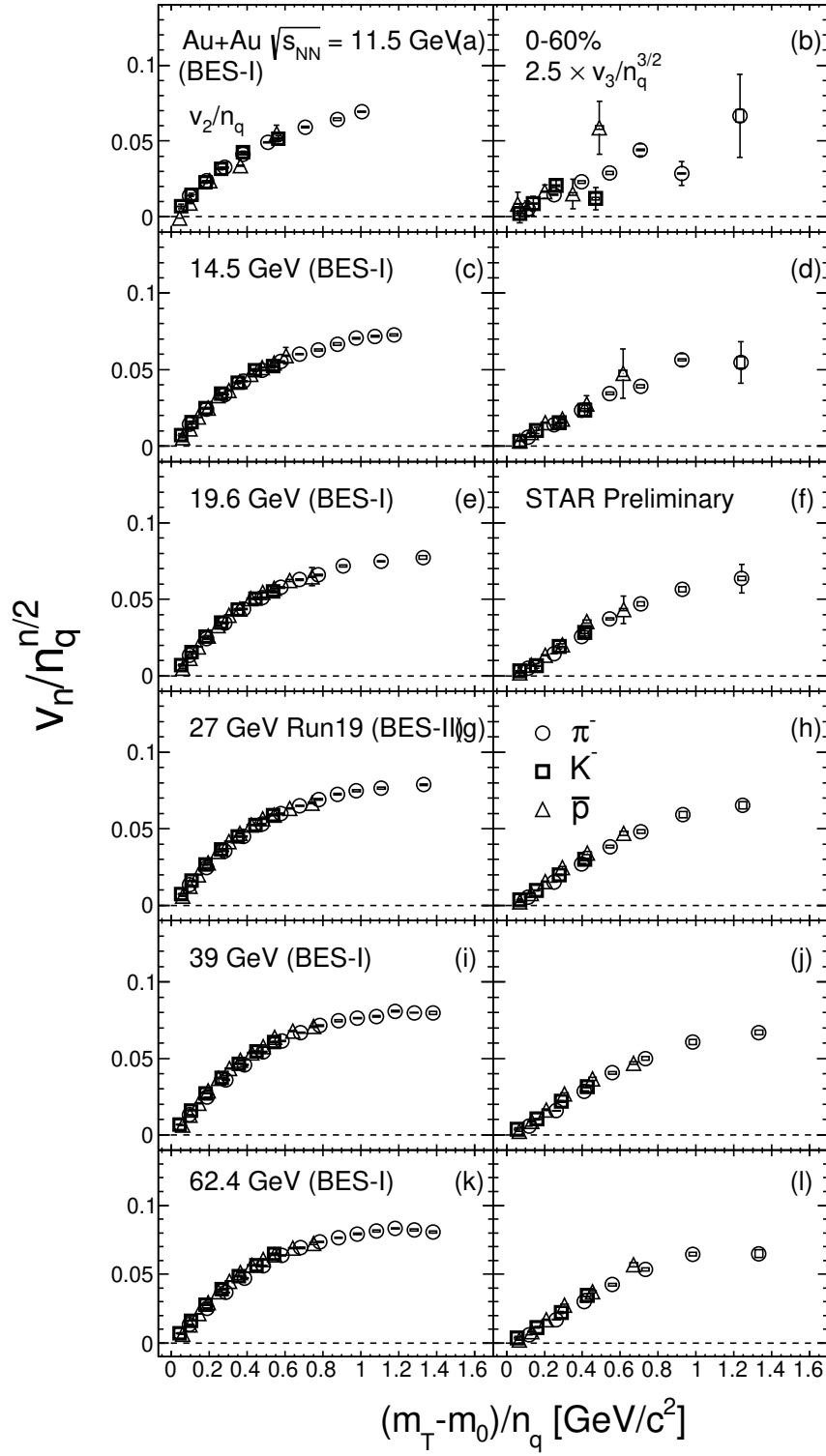


FIG. 6. The number-of-constituent quark (NCQ) scaled v_2 and v_3 of negatively charged particles for 0%-60% central Au+Au collisions and six energies.

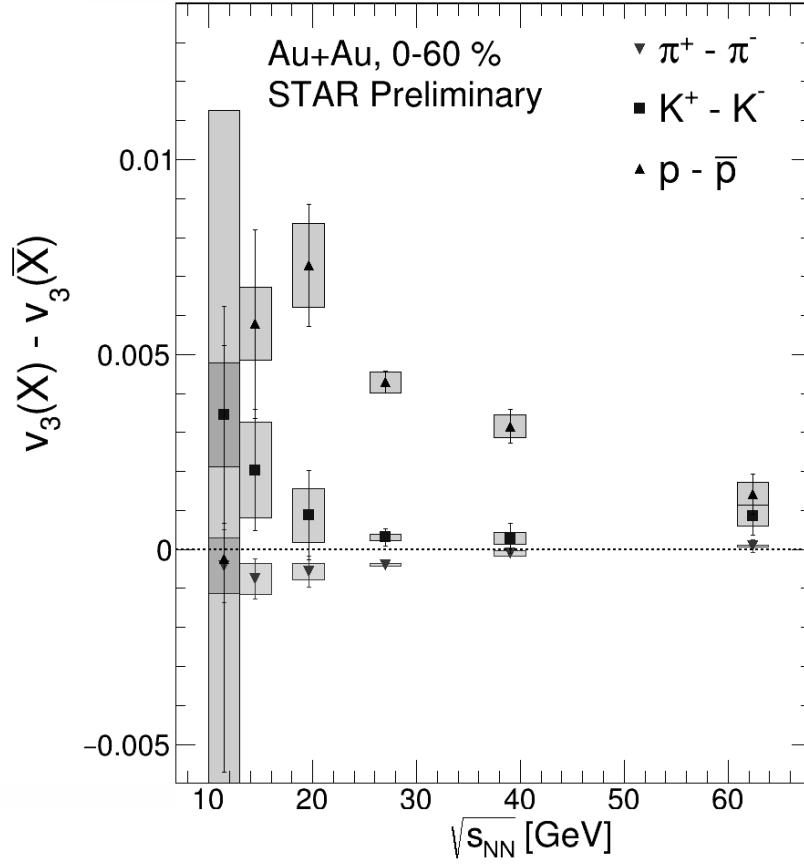


FIG. 7. Difference of triangular flow between positively and negatively charged particles as a function of collisions energy for centrality 0%-60%.

-
- 84 [1] M. M. Aggarwal *et al.* (STAR), (2010), arXiv:1007.2613 [nucl-ex].
- 85 [2] S. Voloshin and Y. Zhang, Zeitschrift for Physik C Particles and Fields **70**, 665–671 (1996).
- 86 [3] A. M. Poskanzer and S. A. Voloshin, Physical Review C **58**, 1671–1678 (1998).
- 87 [4] L. Adamczyk *et al.* (STAR), Physical Review C **98**, 014915 (2018).
- 88 [5] J. Adam *et al.* (ALICE), JHEP **09**, 164 (2016).
- 89 [6] I. Selyuzhenkov and S. Voloshin, Physical Review C **77**, 034904 (2008).
- 90 [7] S. A. Voloshin, A. M. Poskanzer, and R. Snellings, Landolt-Bornstein **23**, 293 (2010).
- 91 [8] C. Adler *et al.* (STAR), Physical Review Letters **89**, 132301 (2002).
- 92 [9] J. Adams *et al.* (STAR), Physical Review Letters **95**, 122301 (2005).
- 93 [10] S. Afanasiev *et al.* (STAR), Physical Review Letters **99**, 052301 (2007).
- 94 [11] B. I. Abelev *et al.* (STAR), Physical Review C **77**, 054901 (2008).
- 95 [12] L. Adamczyk *et al.* (STAR), Physical Review C **88**, 014902 (2013).
- 96 [13] L. Adamczyk *et al.* (STAR), Physical Review C **93** (2016).